Environ Earth Sci (2016) 75:658
DOI 10.1007/s12665-016-5336-8

ORIGINAL ARTICLE

Development of a loess-mudstone landslide in a fault fracture zone

Jianbing Peng[1,2] · Yanqiu Leng[1,2] · Xinghua Zhu[1,2] · Di Wu[1,2] · Xiao Tong[1,2]

Received: 13 April 2015 / Accepted: 6 December 2015 / Published online: 11 April 2016

Abstract A landslide occurred on the morning of December 16, 2013, in Liujiabao village, Tianshui City, Gansu Province, China. The 260,000 m^3 of landslide material traveled a distance of 190 m downslope and damaged a village road and several farmhouses before it stopped on the middle of the slope. These landslide materials are still threatening the lives and property of people in the downslope residential areas. A field survey revealed that this landslide was strongly affected by the geological setting. Six normal faults that extend from east to west developed in the Neogene mudstone of this region; these faults form a fault fracture zone with a width of 80 m. The authors performed a detailed investigation of the geological features of these six normal faults, and their spatial and faulting relationships to the landslide were examined. Finally, the evolutionary progress of the loess-mudstone landslide controlled by the fault fracture zone is discussed.

Keywords Landslide · Fault fracture zone · Loess-mudstone · Flow slide

✉ Jianbing Peng
dicexy_1@126.com

[1] Department of Geological Engineering, Chang'an University, Xi'an 710054, Shaanxi, People's Republic of China

[2] Key Laboratory of Western China Mineral Resources and Geological Engineering, Ministry of Education of the People's Republic of China, Xi'an 710054, Shaanxi, People's Republic of China

Introduction

On December 16, 2013 at 06:00 a.m. local time, a landslide occurred in NW China. The landslide was located on a slope behind Liujiabao village. Liujiabao village is located in Mapaoquan town, Maiji district, Tianshui city, Gansu Province, and is about 20.5 km southeast of the city (location is shown in Fig. 1; this landslide is hereafter termed as Liujiabao landslide, and is shown in Fig. 2a). The displaced rock and soil of the flow slide, with a length of about 100 m, cut the road into two parts, forming a 20-m scarp between these two parts. In addition, the abandoned houses on the north side of the slope were damaged. At present, the slipped mass of Liujiabao landslide is "hanging" on the slope, strongly threatening the safety of the downslope urban residents and industrial premises as well as the expressway (as shown in Fig. 2b).

It is well known that during an earthquake, the introduction of a coseismic force results in the instability of slopes, while during a rainfall event, the decrease in the shear strength of the soil layers and the addition of hydrological forces are the main reasons for the initiation of slope instability (Wang et al. 2007; Sanchez et al. 2010). Therefore, numerous efforts had been made to examine the possible addition of a coseismic force during an earthquake (Nishimura 2009; Zhang et al. 2013, 2015; Shi et al. 2015), the possible reduction of suction in unsaturated soil layers (e.g., Bittelli et al. 2012; Sorbino and Nicotera 2013; Tang et al. 2014), the increase of pore water pressure due to the increase of the ground water table (e.g., Schnellmann et al. 2010; Zhou et al. 2014; Tang et al. 2014), and the hydrological force accompanying the underground water flow (Lourenço et al. 2006; Saada et al. 2012; Cho 2013; Shi et al. 2015). These studies enabled researchers to deepen their understanding of the initiation of many landslides.

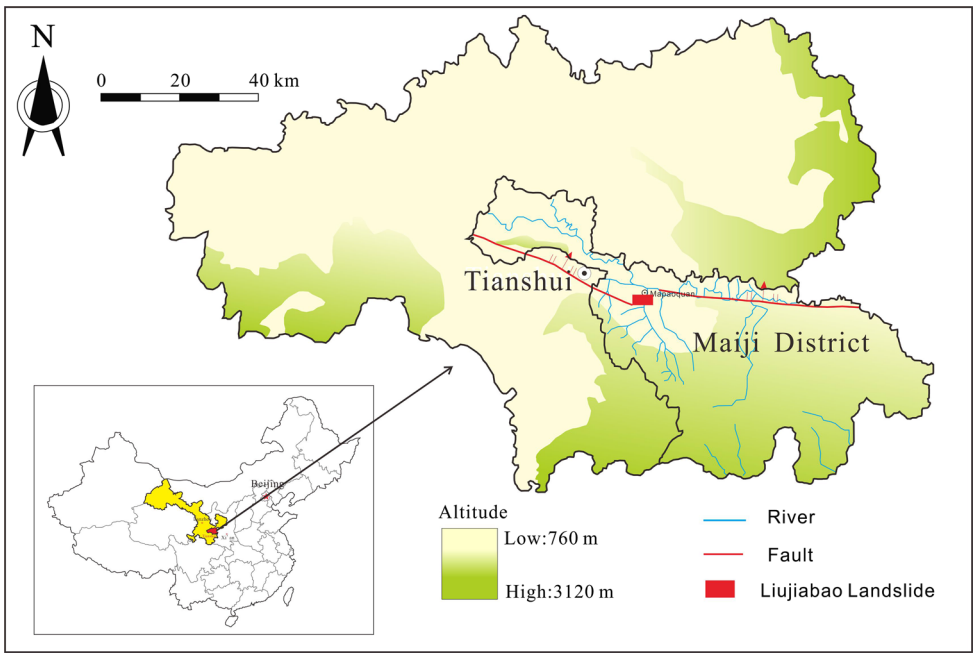

Fig. 1 Location of Liujiabao landslide. Liujiabao landslide is located in Mapaoquan town, Maiji district, Tianshui city, Gansu Province, China

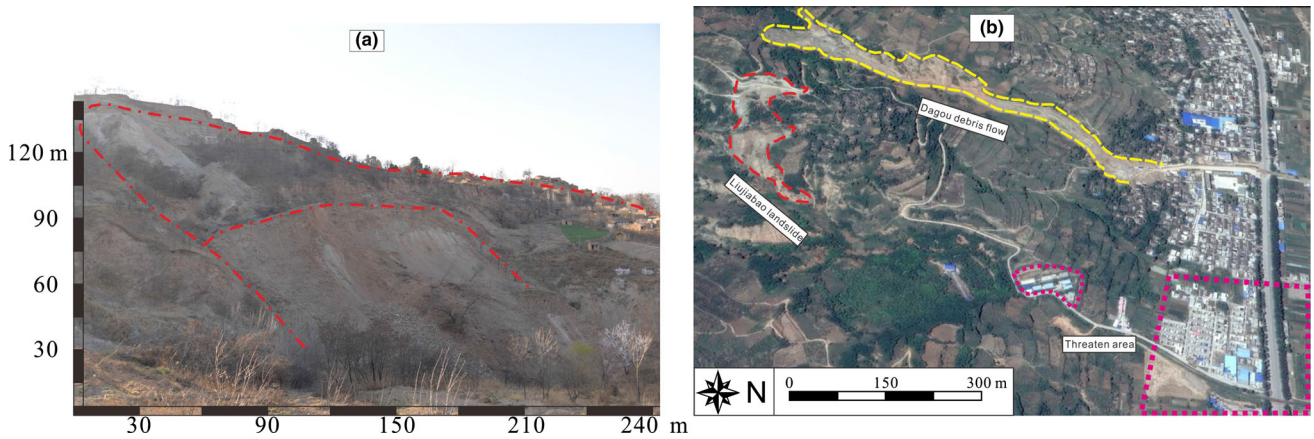

Fig. 2 Macroscopic view of Liujiabao landslide. **a** Oblique front view of Liujiabao landslide. **b** The downslope residential area of Liujiabao landslide (based on satellite imagery captured on 17 June, 2014)

Nevertheless, it still remains to be answered why a landslide occurs on a given slope while the neighboring slopes remain stable, despite the fact that the slopes have approximately the same topography and are subjected to the same co-seismic force or rainfall. Therefore, understanding the geological background of different landslides will be of great importance. However, due to the cost as well as the difficulty in identifying the locations of potential landslides within a large area, detailed examinations of the geological settings of many landslides before their occurrence is not available.

Recently, there have been some studies analyzing landslide occurrence in the context of geological features, and it has been made clear that faulting could be one of the important factors triggering landslides. For example, through field investigation and visual interpretation of high-resolution satellite images, Xu et al. (2014) located at least 2330 landslides triggered by the Minxian–Zhangxian earthquake. According to the authors, the spatial pattern of these co-seismically triggered landslides was strongly controlled by faulting, which indicated the effect of seismogenics and faulting on landslides. Based on the research of Has and Nozaki (2014), most of the landslides induced by the earthquakes were located on the hanging wall of the source fault and were controlled by the geological structures (Kojima et al. 2014). Among these landslides, the slopes perpendicular to the fault extension direction were more prone to the occurrence of landslides, while the typical geological structure, such as the fault, and the bedding plane served as the sliding surface following the strong ground

motion. Meanwhile, the authors also found that some landslides developed along non-tectonic faults, which turned out to be the controlling factor in the occurrence of these landslides. Dill et al. (2012) investigated the anatomy of landslides along the Dead Sea transform fault system (DSTFS); and they found that the movement of the strike fault governed the position as well as the slip direction of the landslides. There were numerous minor and major landslides that developed along the fractures triggered by the movement of the DSTFS. According to the study, almost all of the back scarps of the landslides were derived from extensional or compressional cracks. For the minor landslides, the back scarps were straight and turned into slip planes in the end, while the major landslides had curved back scarps with the sliding direction influenced by the slope direction as well as the fault strike. Combined with a field investigation and digital aerial photographs, Tang et al. (2015) analyzed the types, sizes, and positions of landslides induced by the Lushan Earthquake in China. These authors found that the common types of landslides in the study area were rock falls and shallow, disrupted landslides within the weathered bedrock and colluvium. However, in contradiction to what has been reported in other earthquake areas such as the Wenchuan area (Huang 2009), the location of the hanging wall and the footwall of the fault did not seem to have a strong effect on the landslide distribution resulting from the Lushan Earthquake. Khorsandi and Ghoreishi (2013) studied the interaction between active faults and landslide phenomena. Their results showed that a crushed and mylonitized zone formed by the active fault was the main location of a landslide. In addition to this, the fault also influenced the groundwater table, and resulted in poor water permeability and inadequate drainage of the landslide material, which turned out to be unfavorable conditions for the occurrence of a landslide.

However, these landslides were triggered immediately after the earthquake or rainfall. In the current study, a landslide that occurred in Liujiabao village, Tianshui, Gansu Province, China, is presented. This landslide occurred without any directly related trigger. Through detailed field investigation, the authors found that there are six normal faults in the Neogene mudstone on the back scarp of the landslide, which had the same east–west trend (parallel to the sliding direction). These faults formed an 80-m wide fracture zone, which accounted for 2/3 of the back scarp width of the landslide. It is inferred that this landslide was mainly controlled by its geological structures. This study aims to: (1) clarify the geological characteristics of these faults; (2) identify the spatial relationships between these faults and the landslide debris; and (3) discuss the evolutionary progress of the loess-mudstone landslide controlled by these faults.

Geological setting of Liujiabao landslide

As shown in Fig. 3a, Tianshui is located in the southwestern region of the West Gansu loess plateau, and it is adjacent to West Qinling Mountain and Fenwei Basin on the south and west sides, respectively. This region belongs

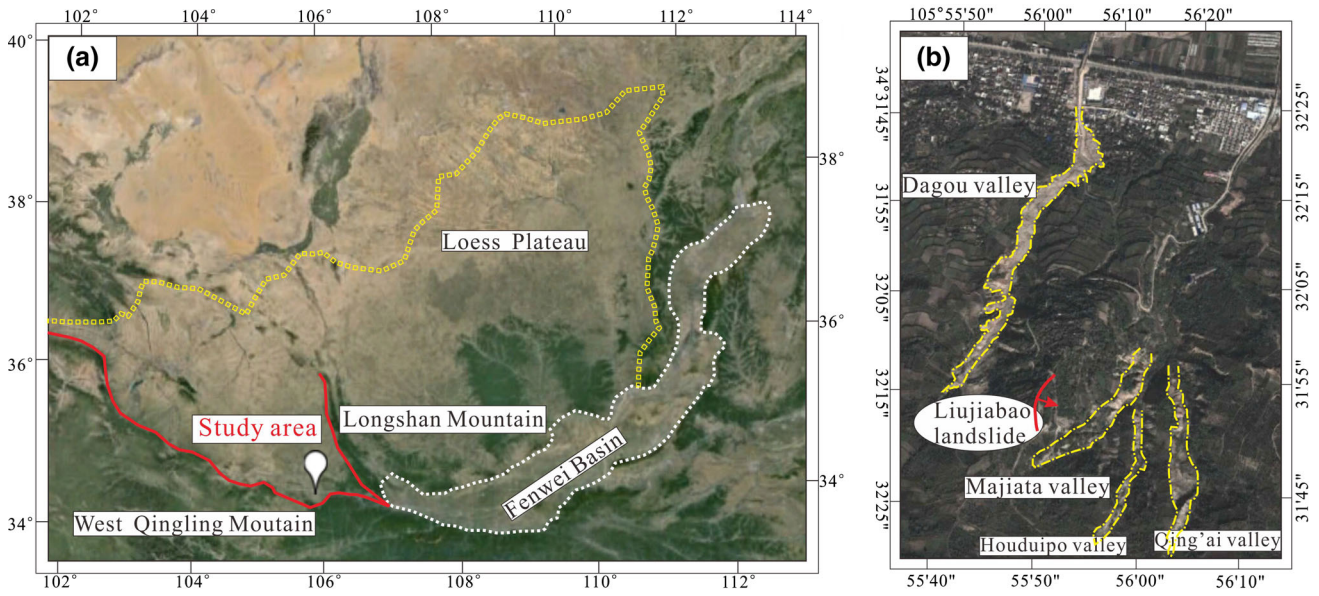

Fig. 3 Location of the Tianshui area and Liujiabao landslide. **a** Tianshui is located in the southeastern part of the west Gansu loess plateau and is adjacent to West Qinling Mountain and the Fenwei Basin. **b** Liujiabao landslide occurred in a loess area with gully-hilly topography (based on satellite imagery captured on 19 October, 2013)

to the hilly geomorphic section of the loess plateau, with its terrain characterized by a high northeastern region and a low southwestern region (Fig. 3b). Liujiabao village is located southwest of the Maiji district, Tianshui, which is characterized by loess with a gully-hilly topography. Liujiabao landslide developed in loess with hilly terrain and a northeast-southwest trend. The ridge undulates greatly in height; that is, it is low in the northern region and high in the southern region with an average slope of about 60°. This steep slope makes it much easier for landslides to occur. Four valleys developed on the eastern and western sides of Liujiabao landslide; from west to east these valleys are Dagou valley, Majiata valley, Houduipo valley, and Qing'ai valley. Dagou valley is located on the western side of the loess ridge, and it is the locality of the Dagou debris flow, as mentioned previously. The other three valleys are on the eastern side of the loess ridge. Liujiabao landslide occurred upstream of Majiata valley. As can be seen from Fig. 3b, it is clear that Majiata valley first converges with Houduipo valley, and then it merges with Qing'ai valley half way along its length.

Tianshui lies in the transition zone between Qinling Mountain and Longshan Mountain (as shown in Fig. 3a). Therefore, many deep faults have developed, neotectonic movement is intense, and earthquakes are frequent in this region (Teng et al. 1994). Influenced by the levorotation extension of the Obrdos platform, several deep faults developed along West Qinling Mountain, creating the fault zone at the northern edge of West Qinling Mountain (as shown in Fig. 4a). This fault zone, which starts at Baoji city in the east, passes by Tianshui city, Wushan, and Zhangxian county and arrives in Tongren county, Qinghai province, and can be divided into about 6 secondary fault zones of unequal sizes. According to Shao et al. (2011), these are the Baoji–Tianshui fault (F_1 in Fig. 4a), the Tianshui–Fenghuang fault (F_2), the Wushan fault (F_3), the Zhangxian fault (F_4), the Huangxianggou fault (F_5), and the Guomatan fault (F_6), which form a combination sinistral echelon. As the study of Cheng et al. (2009) shows, the West Qinling Mountain fault zone has an average strike of 280°–310° but twists in some places, and all the faults have a NE trend, with dip angles ranging from 50° to 70°. This normal fault zone has a sinistral strike-slip component. As shown in Fig. 4a, Liujiabao landslide is situated on the hanging wall of the F_2 fault, and the deformation caused by the fracture's extension has loosened the rock and soil mass; thus, many secondary faults have developed there. In Fig. 4b, it can be seen that 6 normal faults with similar strike and trend have developed at the back scarp of Liujiabao landslide. All the faults have a southward trend, which has resulted in the decrease of the mudstone layers and a fracture zone 80 m wide. Within the fracture zone,

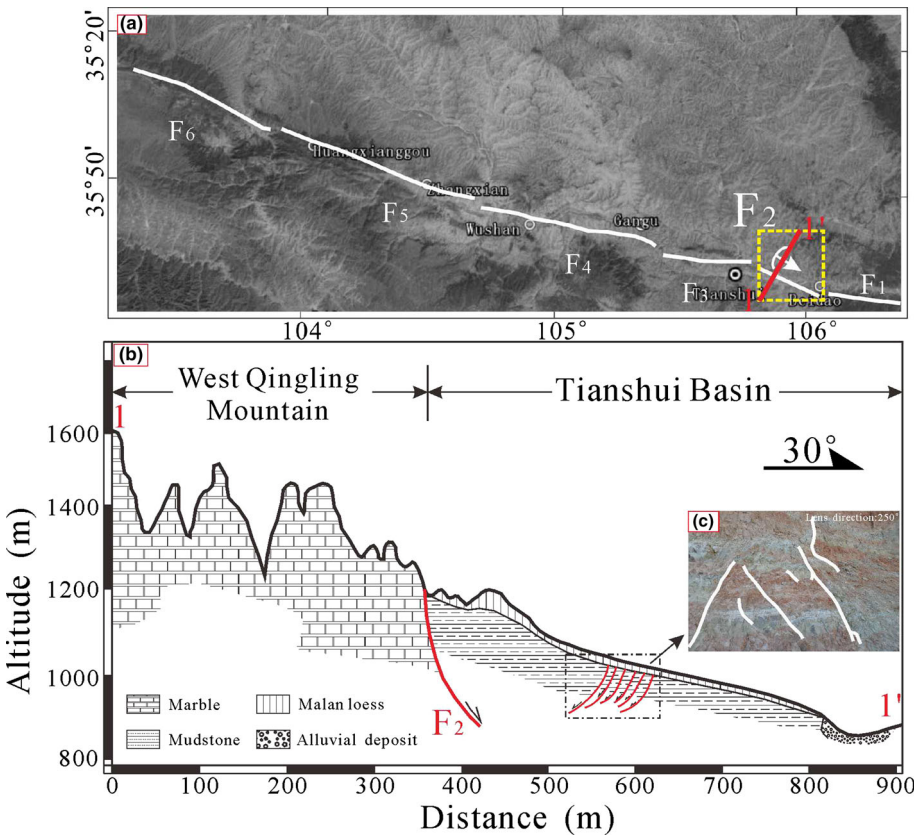

Fig. 4 Geologic section map of the secondary faults on the hanging wall of the West Qinling fault. **a** The landslide is located on the hanging wall of the Tianshui–Fenghuang fault; **b** secondary faults with the same southward trend developed here, dislocating the Neogene mudstone; and **c** secondary faults as well as joints developed within the fault zone cutting the mudstone into a fragmented texture

there are many small faults as well as joints cutting the mudstone into a fragmented texture, as shown in Fig. 4c.

The underlying stratum is a thick layer of soft Neogene (N) mudstone, which acts as the slope basement. Then the wind deposited a layer of Pleistocene (Q_3) loess (Malan loess) on top of the mudstone (Sun 2005). Finally, a thin layer of Holocene (Q_4) loose loess precipitated on the surface of the Malan loess. The strata here are Neogene mudstone, Malan loess and Holocene loess from old to new, as shown in Fig. 5. The loose loess deposited in the Holocene is about 1–2 m thick and covers the slope surface. With respect to the composition, it is mainly composed of silty clay and sand as well as cobble-sized gravel. The surficial Malan loess is about 3–7 m thick with an average thickness of 4 m and is characterized by a loosened structure, high void ratio, and abundant vertical joints. The Malan loess contact with the underlying Neogene mudstone is an unconformity. Influenced by weathering and fault stretching, the growth of joints in the Neogene mudstone makes it soft and loose, especially when wet (as the experimental data show).

The climate here belongs to a type of semi-arid continental monsoon climate, with uneven rainfall. The highly disturbed and fractured geologic setting combined with an originally adverse natural climate provide favorable conditions for geologic disasters, which makes Tianshui one of the cities in China that is prone to geologic disasters. More than 300 large-scale geologic disasters have occurred in Tianshui, and the slope damage ratio along both the southern and northern sides of the city is as high as 50 % (Wu and He 2003). For example, a recent landslide that occurred in Dagou village, Tianshui, in July 2013 resulted in extensive damage to the downslope residential area (Peng et al. 2014).

Liujiabao landslide

Geomorphic characteristics

Liujiabao landslide is located in a loess area with a gully-hilly topography. Figure 5 shows the contour map and 3-D

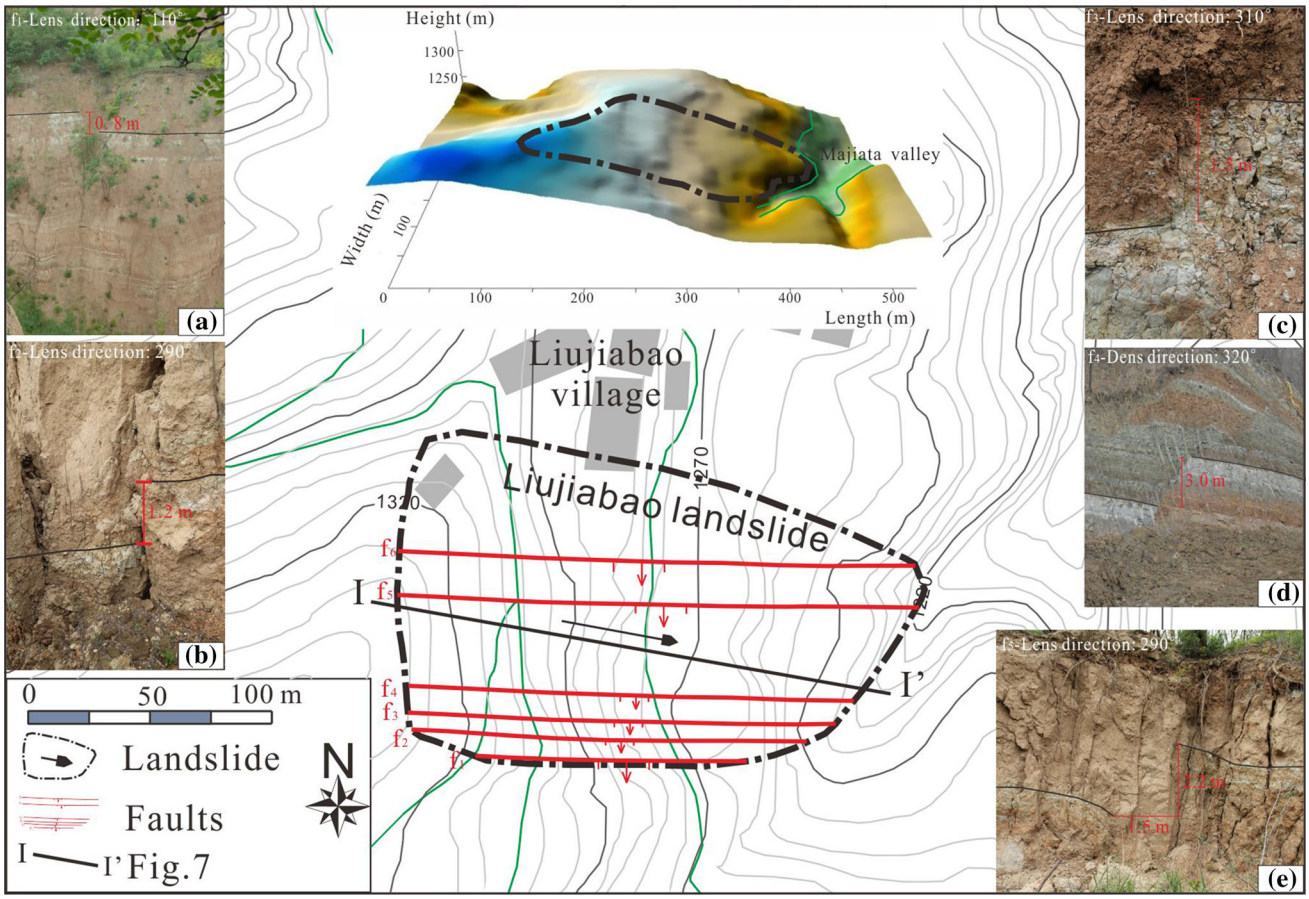

Fig. 5 Contour map and 3-D topography of the area before the Liujiabao landslide occurred. Inside the landslide area, there were six normal faults. **a** The outcrop of the f_1 fault was located in Majiata valley; **b** the f_2 fault was exposed on the scarp situated in the middle of the slope; **c** the f_3 fault was about 6 m north of the f_2 fault; **d** the excavation of the road, which was located to the west of Liujiabao landslide, made the f_4 fault visible; and **e** the f_5 fault was located on the same scarp as the f_3 fault but was located 45 m to the north

topography before the landslide occurred. The slide area, which is marked in Fig. 5, is about 50,000 m^2, 230 m in length (measured from the back scarp to the leading edge) and 225 m in width. On the contour map, it is clearly seen that the elevation of the shear opening is 1210 m, with the leading edge ranging from 1210 to 1255 m and the trailing edge ranging from 1300 to 1350 m, which results in an average height difference of about 110 m. The slip direction is 100° SE, and along this slip direction, the rock and soil debris moved downwards, eventually packing into the valley at the toe of the slope.

The trailing edge of Liujiabao landslide lies on the loess ridge, while the leading edge is situated in Majiata valley; and both the trailing edge and the leading edge are covered by unconsolidated sediments. The landslide area is shown (Fig. 5) as a convex irregular quadrangle in the plane with an upper part that is 228 m wide and a lower part that is 103 m wide. There are 6 normal faults with an E–W trend in this area, and most of the slip mass developed within the 80-m wide fault fracture zone. Liujiabao landslide shares a southern boundary with fault f_1. Neogene mudstone, with the occurrence of 300°∠4°, is exposed on the eastern side of Majiata valley. The inclination of the mudstone layer is close to zero, but its trend is opposite to the slide direction.

Deformation partition

According to a field investigation, the current situation of Liujiabao landslide was caused by two sliding processes and a creeping process. Based on the stability of the slope and its motion characteristics, Liujiabao landslide can be divided into two zones, sliding zone A and creeping zone B, as shown in Fig. 6. According to the deformation signs, sliding zone A was the first zone to fail during its deformation process; while creeping zone B, which is located to the north of zone A, was dragged by creep deformation.

Sliding zone A was located in the southern part of the landslide, and a normal fault served as the southern boundary of the landslide. The width of zone A's back scarp was about 120 m, and using the artificial scarp at the middle of the slope, it can be divided into zone A-1 and zone A-2. Zone A-1 belonged to the upper part of the slope and was the main slide zone. In addition, in the sliding direction, Fig. 6a shows that there was a group of steps descending from the center to the margo lateralis of the landslide. Zone A-2 is located to the east of zone A-1. In this area, the slip mass was 6–8 m thick and was mainly composed of loess-like soil and gravely soil. Figure 6b shows pictures of the leading edge of zone A-2, in which it is clear that the debris mass is mainly composed of loess-

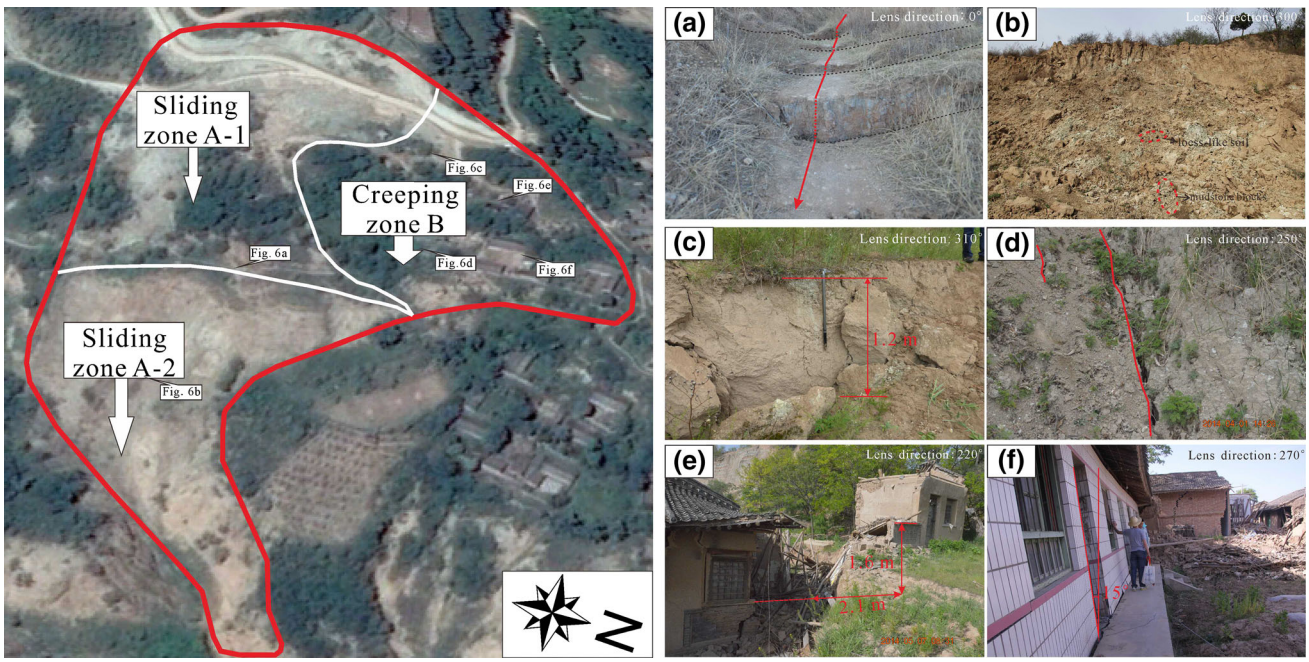

Fig. 6 Partition map of Liujiabao landslide (drawn from the satellite image captured on 17 June, 2014). The landslide can be divided into two sliding zones and a creeping zone according to the different motion characteristics. The basic characteristics of sliding zone A are as follows: **a** a group of steps descending from the center to the margo lateralis in zone A-1; and **b** the debris mass in zone A-2 is mainly composed of loess-like soil and mudstone blocks. The typical features of the creeping zone B are as follows: **c** A 1.2-m staggered slab was formed by the extension crack trending S–N; **d** Radial cracks at the leading edge trended E–W with a stretch width of 3–5 cm; **e** Influenced by the extension crack, a house suffered a 2.1-m horizontal displacement and a 1.6-m *vertical offset*; and **f** creep deformation of the free face resulted in a house lying on its back and formed a 15° angle with the *vertical direction*

like soil as well as mudstone blocks, whose diameters range from several centimeters to tens of centimeters.

Creeping zone B is located to the north of sliding zone A. Its floor area was about 0.001 km^2, with a length of 110 m and a width of 90 m. Creeping zone B was dragged by zone A, and since it was concentrated in a residential area, it was the worst-hit area when the landslide happened. A tension crack, extending from north to south, developed on the trailing edge of creeping zone B and created a staggered 1.2-m slab, as shown in Fig. 6c. Meanwhile, blocked by the slope located to the east, the leading edge of zone B developed a group of radial cracks extending from east to west (as shown in Fig. 6d). The radial cracks stretched for more than 10 m, and their widths ranged from 3 to 5 cm. About ten abandoned houses in this region suffered varying degrees of damage, and as such, they either had a horizontal displacement along with vertical offset (Fig. 6e), or lay on their own backs (Fig. 6f). Since it was characterized by creep deformation, this region was named the creeping zone.

Slip mass and its motion characteristics

A longitudinal section along line I–I′ (shown in Fig. 5) is shown in Fig. 7. The present ground surface was measured using a hand-held laser rangefinder during our investigation. The surface of the slip mass waved up and down at a steep angle; hence, it is now semi-hanging on the slope in an unstable state. In the middle of the slope, there was a village road that extended from north to south. The slip mass can be divided into two platforms with two steep slopes from top to bottom, and the height of the steep slope is about 10–15 m, while the average slope angle is 65°. In addition, there are some drumlins composed of either crushed mudstone or secondary accumulation on the surface of the landslide.

As mentioned before, there were two sliding zones. Zone A-1 was the main sliding zone, and it descended a vertical distance of 46 m over a horizontal distance of 113 m. Zone A-2 was located on the lower part of the slope body, and it descended a vertical distance of 44 m over a horizontal distance of 77 m. The displaced materials from the source area have an estimated volume of 26.5×10^4 m^3. Zone A-1 had a relatively slow moving surface; therefore, the slip mass materials were sheared out at the weak plane in a slow surge sliding motion (as shown in Fig. 7a). Compared with zone A-1, zone A-2 had a steeper surface and it mainly moved in a quick slipping motion (as shown in Fig. 7b).

According to the investigation and Fig. 7c, the slip mass materials were all sheared out at the soft mudstone layer. The high-steep trailing segment of the slip surface was excavated into the back scarp of Liujiabao landslide. Apart from the back scarp, all parts of the slope surface were covered by loose landslide deposits, which were mainly composed of loess-like soil and mudstone fragment. The loess-like soil was yellowish-brown and was mainly composed of fine particles, while the mudstone was greyish-green with an average grain diameter of 5–25 cm and a

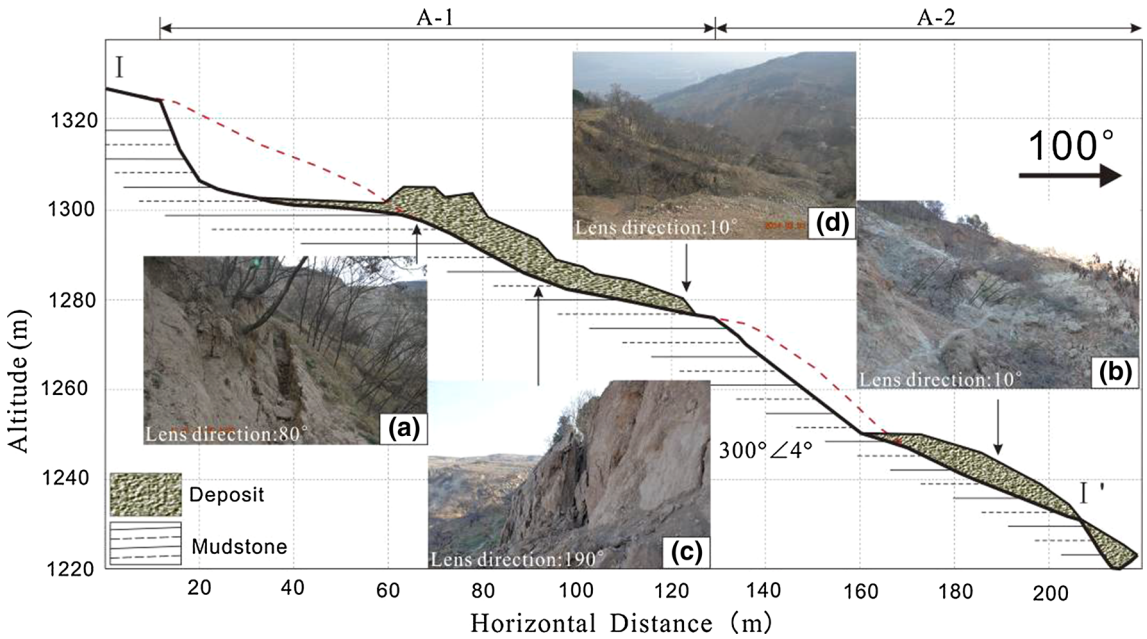

Fig. 7 Motion features of Liujiabao landslide, such as: **a** surge sliding motion in zone A-1 and **b** quick slip motion in zone A-2. Longitudinal section along line I–I′ as shown in Fig. 5: **c** the slope body was sheared out at the mudstone in zone A-1 and **d** the sorting of the slip mass was good in the plane

maximum diameter of 50 cm. The original rock sequence of the slip mass was disordered: on the one hand, mudstone fragments were overhead and overlapped with loess-like interleaved soil; while on the other hand, mudstone fragments were distributed in the front and middle of the slope with a thickness of 3–5 m, and loess-like soil was distributed in the posterior with a thickness of 10 m in zone A-1 and 6–8 m in zone A-2, as shown in Fig. 7d.

Structural features of the slide bed and back scarp of Liujiabao landslide

The slide bed of Liujiabao landslide was composed of Neogene mudstone, and it trended 300° NE, which was contrary to the slope trend, with an inclination angle of only 4°. Malan loess cut through the approximately horizontal mudstone layer and then formed an in sequent landslide. The back scarp was located on the loess ridge extending from north to south, and its altitude and width were 1320 and 120 m, respectively. According to Fig. 8a, an 80-m wide fault zone was uncovered at the back scarp of Liujiabao landslide. There were 6 normal faults within the fault zone and they were named f_1–f_6 in Fig. 8b.

In the plane, as shown in Fig. 5, fault f_1 was located in the south and defined as the southern boundary of Liujiabao landslide. The horizontal spacing between f_2 and f_1 was 8 m, and a small-scale fault f_1' developed between them. Fault f_3 was approximately parallel to f_2, and the spacing between them was 6 m. Faults f_3–f_6 are arranged from south to north successively, and spacing between the adjacent faults was 11, 35, and 18 m.

In profile, all the faults except f_1' trended 190°SW with inclination angles ranging from 60° to 65°; whereas fault f_1' trended 10°NE with an inclination angle of 65°. Fault f_1, f_1', and f_2 moved the red mudstone 1.5, −0.5, and 2.2 m, respectively, down and to the south (minus indicates to the north). Fault f_3 was steeper at its bottom than at its top, and it dislocated not only grey-white but also red mudstone by 2.0 m. Meanwhile, fault f_3 also formed traction structures at both walls of the fault. Since fault f_4 formed 3.3- and 4.0-

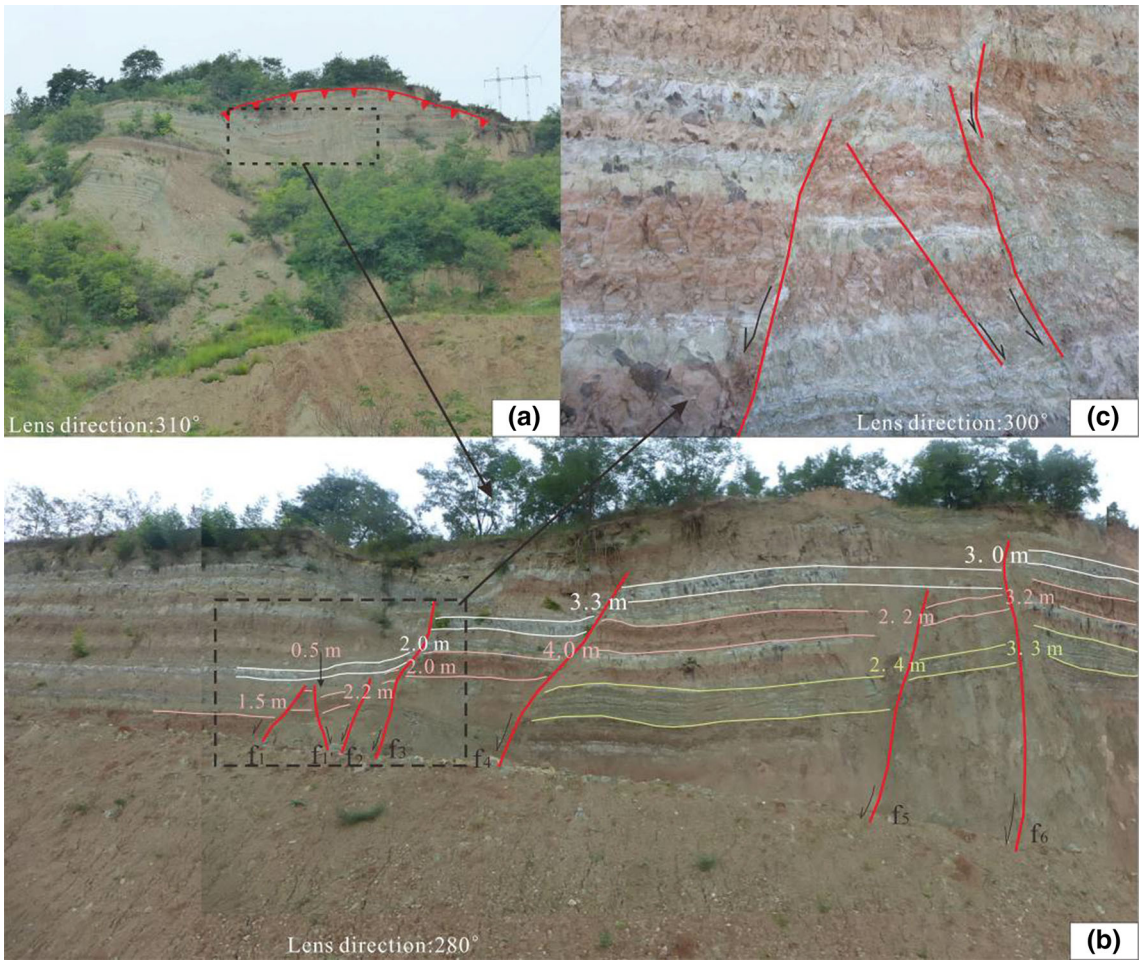

Fig. 8 Back scarp and fault section of Liujiabao landslide. **a** The width of the back scarp was 120 m, while the width of the fault fracture zone was 80 m. **b** 6 Normal faults developed within the fault fracture zone. **c** Mudstone was cut into pieces due to the development of secondary faults

m offsets in the grey-white and red mudstone, respectively, it became the fault with the biggest offsets within the fault zone. Fault f_5 showed a vertical shape in profile, and it cut red and grey-green mudstone from its top to its bottom, with a 2.2-m displacement. Parallel to f_5, fault f_6 dislocated grey-white, red, and grey-green mudstone from top to bottom, with displacements of 3.0, 3.2, and 3.3 m, respectively, which indicates a co-depositional activity characteristic.

The faults mentioned above were active in stages; therefore, their controlling effects on Liujiabao landslide were not the same. Faults f_1, f_1', f_2, and f_5 did not cut the grey-white mudstone at the bottom; therefore, they formed at an earlier age. In addition, all four faults had smaller displacements (the maximum was only 2.4 m), but they did cause the intense crushing of rock and soil, as Fig. 8c shows. Fault f_1 defined the southern boundary of Liujiabao landslide and played an important role in the occurrence of the landslide. Faults f_3, f_4, and f_6 are larger and had bigger displacements (the maximum reached 4.0 m). These three faults cut the grey-white mudstone and were accessible to the near surface. It was assumed that they belonged to the secondary active faults located on the hanging wall of the northern margin fault zone in Qinling Mountain, and that they were persistently active in recent years (Cheng et al. 2007). According to a disaster report from the local government in 2008 after Wenchuan Earthquake (http://www.gsdlr.gov.cn), the movement of these faults had already provided dynamic conditions for the initiation and formation of Liujiabao landslide.

Discussion

Based on the preceding analysis, Liujiabao landslide was a loess-mudstone landslide that occurred along a fault fracture zone, and its formation was closely related to the frail geological environment (Xin et al. 2012) . Under the influence of all of the geological and geomorphological factors mentioned above, the Liujiabao slope began to creep downward after the Wenchuan earthquake; thus, the local government began to move the threatened residents downhill (reported by http://www.maiji.gov.cn in 2009). After the last long heavy rain in July 2013, the large amount of rainfall infiltrated along joints and fault fractures, soaking, lubricating, and eventually weakening the mudstone.

Therefore, it is inferred that the evolutionary progress of a landslide that developed along a fault fracture zone could be as follows.

Step 1: the embryonic stage. Several normal faults developed in the slope, breaking the Neogene mudstone into a fracture zone, whose extension direction was consistent with the slope of the ridge. Then, a thin layer of loess covered the thick mudstone, but it was not subsequently cut through by the fault. Hence, the slope was in an East–West tensional stress field, which was more prone to create an unstable slope, as Fig. 9a shows. Step 2: the creep cracking stage. During the 2008 Wenchuan Earthquake, the slope suffered from a horizontal seismic force (as the red arrow shows in Fig. 9b), which produced the resultant force that caused

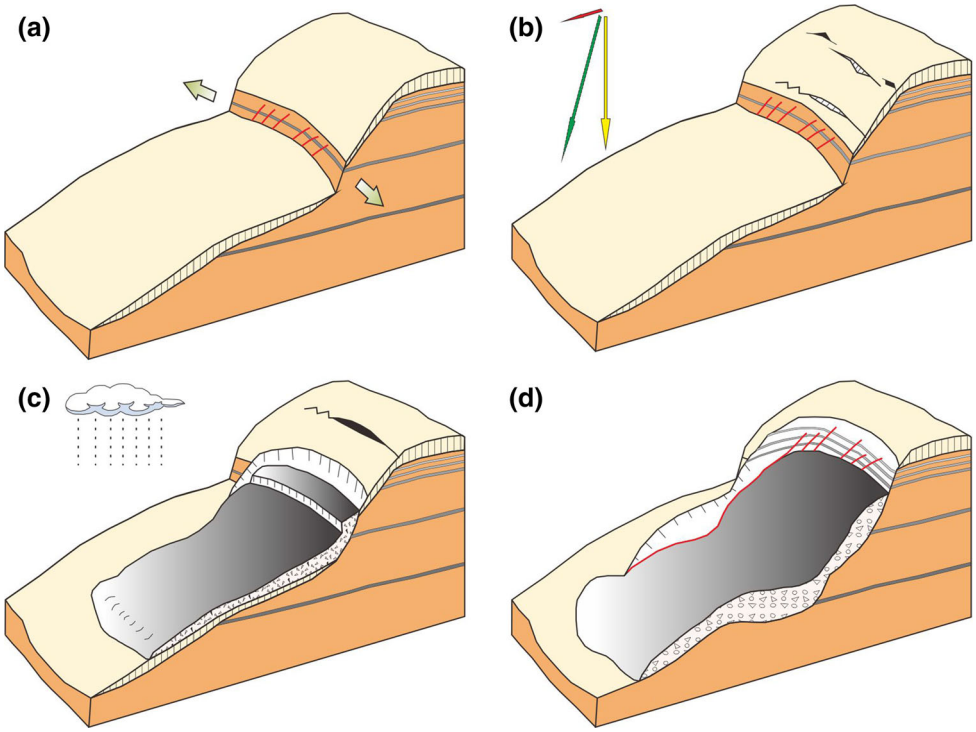

Fig. 9 Evolution model of Liujiabao landslide. **a** A fault fracture zone developed along the slope direction. **b** Extension cracks emerge on the creeping slope after the earthquake. **c** The slope begins to slip during rainfall. **d** With the infiltration of rainfall, the slope starts to slide until it is in a semi-hanging state

the slope to rotate (as the green arrow shows in Fig. 9b). In addition, Quaternary neotectonic movement triggered the active faults in this area, dislocating the layers. Then, tension cracks emerged on both the upper and middle parts of the slope. That is, the Wenchuan Earthquake in 2008 aggravated the overall deformation of the Liujiabao slope.

Step 3: the sliding stage. In July 2013, the last long heavy rain resulted in large amounts of rainfall that seeped into the slope and weakened the strength of the rock and soil. Hence, the middle part of the slope started to slip, and the extension cracks kept on expanding until the sliding is through to the surface (shown in Fig. 9c).

Step 4: the present stage. After the locked patch loses its stability, the upper part of the slope begins to slide along the cracks. The slip mass is semi-hanging on the slide bed, and the fault zone is exposed on the back scarp of the landslide, as Fig. 9d shows.

Due to the effect of tensile in situ stress, secondary faults develop easily on the hanging wall of a large fault. In the study area, the slope was high in the east and low in the west with an average slope angle of about 65°, and the strata were composed of loess and mudstone. The strike of the secondary faults developed in this area was EW. Generally speaking, there were two kinds of weak structural planes, i.e., loess mudstone interfaces (named the primary structural plane) and the fault plane (named the geological structural plane), existing within the slope body, and they were perpendicular to each other. Under the influence of the neotectonics, seismic force, and the climatic conditions, the primary structural plane rather than the geological structural plane became the main factor controlling the stability of the slope.

Summary and conclusions

On December 16th, 2013, a rock-soil debris landslide occurred in Liujiabao village in the northwestern part of China. The landslide slid in an E–W direction, and it finally formed nearly 26×10^4 m^3 of loess-mudstone deposits.

1. Secondary faults that developed on the hanging wall of the fault zone at the northern edge of West Qinling Mountain produced an 80-m wide fault fracture zone containing 6 normal faults. Liujiabao landslide originated along the fault fracture zone but was a little wider (120 m wide) than the fault zone.
2. Though both the primary structural plane and the geological structural plane existed within the Liujiabao slope, the slip direction was controlled by the primary structural plane, with the normal fault located to the south, controlling the southern boundary of this landslide.
3. Liujiabao landslide was affected by the loess-mudstone strati-graphic association model, faulting in the fault fracture zone, seismic force, and concentrated rainfall infiltration. This kind of geologic setting and climate conditions are common in northwestern China, thus providing favorable conditions for large-scale landslides in this area.

Finally, it is noted that seismic force, active faults, the geologic setting, and climatic conditions normally affect the frequency and scale of landslides and debris flows. Consequently, the nearby residents live with the possibility of the occurrence of these disasters. Although local people have noticed the damage that geologic disasters bring to their lives and work, they can do nothing when they occur. Hence, detailed research on landslides as well as debris flows that develop within fault fracture zones is of great importance in helping people recognize and prevent potential disasters. Therefore, this research will be helpful in the mitigation of geohazards and the losses caused by them in China.

Acknowledgments This study is funded by the Grant of the Key Program of the National Natural Science Foundation of China (No. 41130753), and the National Basic Research Program of China (973 program) (No. 2014CB744700).

References

Bittelli M, Valentino R, Salvatorelli F, Rossi P (2012) Monitoring soil-water and displacement conditions leading to landslide occurrence in partially saturated clays. Geomorphology 173–174:161–173

Cheng YX, Zhang J, Du DJ (2007) On the relationship between fault activity and geological hazard in Tianshui area, Gansu Province. J Eng Geol 15(01):33–37 **(in Chinese)**

Cheng YX, Zhang J, Liu YJ (2009) Analysis on the feature and radon survey result of the main active faults in Tianshui area. Coal Geol Explor 37(3):5–9 **(in Chinese)**

Cho SE (2013) Probabilistic stability analysis of rainfall-induced landslides considering spatial variability of permeability. Eng Geol 171:11–20

Dill HG, Hahne K, Shaqour F (2012) Anatomy of landslides along the Dead Sea Transform Fault System in NW Jordan. Geomorphology 141–142:134–149

Has B, Nozaki T (2014) Role of geological structure in the occurrence of earthquake-induced landslides, the case of the 2007 Mid-Niigata Offshore Earthquake, Japan. Eng Geol 182:25–36

Huang RQ (2009) Mechanism and geomechanical models of landslide hazards triggered by Wenchuan 8.0 Earthquake. Rock Mech Eng 28:1239–1249 **(in Chinese)**

Khorsandi A, Ghoreishi SH (2013) Studying the interaction between active faults and landslide phenomenon: case study of landslide in Latian, Northeast Tehran, Iran. Geotech Geol Eng 31:617–625

Kojima S, Nagata H, Yamashiroya S, Iwamoto N, Ohtani T (2014) Large deep-seated landslides controlled by geologic structures: prehistoric and modern examples in a Jurassic subduction–

accretion complex on the Kii Peninsula, central Japan. Eng Geol 186:44–56

Lourenço SDN, Kyoji S, Fukuoka H (2006) Failure process and hydrologic response of a two layer physical model: implications for rainfall-induced landslides. Geomorphology 73:115–130

Nishimura T (2009) Slip distribution of the 1973 Numuro-oki earthquake estimated from the re-examined geodetic data. Earth Planets Space 61:1203–1214

Peng JB, Fan ZJ, Wu D, Zhuang JQ, Dai FC, Chen WW, Zhao C (2014) Heavy rainfall triggered loess-mudstone landslide and subsequent debris flow in Tianshui, China. Eng Geol 186:79–90

Saada Z, Maghous S, Garnier D (2012) Stability analysis of rock slopes subjected to seepage forces using the modified Hoek–Brown criterion. Int J Rock Mech Min Sci 55:45–54

Sanchez G, Rolland Y, Corsini M, Braucher R, Bourlès D, Arnold M, Aumaître G (2010) Relationships between tectonics, slope instability and climate change: cosmic ray exposure dating of active faults, landslides and glacial surfaces in the SW Alps. Geomorphology 117:1–13

Schnellmann R, Busslinger M, Schneider HR, Rahardjo H (2010) Effect of rising water table in an unsaturated slope. Eng Geol 114:71–83

Shao YX, Yuan YY, Wang AG, Liang MJ, Liu K, Feng JG (2011) The segmentation of rupture and estimate of earthquake risk along the north margin of Western Qinling fault zone. Seismol Geol 33(1):79–90 **(in Chinese)**

Shi ZM, Wang YQ, Peng M, Guan SG, Chen JF (2015) Landslide dam deformation analysis under aftershocks using large-scale shaking table tests measured by videogrammetric technique. Eng Geol 168:68–78

Sorbino G, Nicotera MV (2013) Unsaturated soil mechanics in rainfall-induced flow slide. Eng Geol 165:105–132

Sun JZ (2005) Loessology. Hong Kong archaeological society, Hong Kong **(in Chinese)**

Tang MG, Xu Q, Huang RQ (2014) Site monitoring of suction and temporary pore water pressure in an ancient landslide in the Three Gorges reservoir area, China. Environ Earth Sci 73:5601–5609

Tang C, Ma GC, Chang M, Li WL, Zhang DD, Jia T, Zhou ZY (2015) Landslides triggered by the 20 April 2013 Lushan earthquake, Sichuan Province, China. Eng Geol 187:45–55

Teng RZ, Jin YQ, Li XH, Su XZ (1994) Recent activity characteristics of the fault zone at northern edge of Western Qinling MT. Northwest Seismol J 16:85–90 **(in Chinese)**

Wang HB, Kyoji S, Xu WY (2007) Analysis of a spatial distribution of landslides triggered by the 2004 Chuetsu earthquakes of Niigata Prefecture, Japan. Nat Hazards 41:43–60

Wu WJ, He BY (2003) The problem of environmental geology in Tianshui city. J Gansu Sci 15:200–205 **(in Chinese)**

Xin CL, Yang GL, Zhao ZP, Sun XH, Ma WY, Li HR (2012) Geohazard types and causes analysis in Tianshuishi Beishan. Chin J Geol Hazard Control 23(2):89–95 **(in Chinese)**

Xu C, Xu XW, Shyu J, Bruce H, Zheng WJ, Min W (2014) Landslides triggered by the 22 July 2013 Minxian-Zhangxian, China, Mw 5.9 earthquake: inventory compiling and spatial distribution analysis. J Asian Earth Sci 92:125–142

Zhang YB, Chen GQ, Zheng L, Li YG, Wu J (2013) Effects of near-fault seismic loadings on run-out of large-scale landslide: a case study. Eng Geol 166:216–236

Zhang YB, Zhang J, Chen GQ, Zheng L, Li YG (2015) Effects of vertical seismic force on initiation of the Daguangbao landslide induced by the 2008 Wenchuan earthquake. Soil Dyn Earthq Eng 73:91–102

Zhou YF, Tham LG, Yan WM, Dai FC, Xu L (2014) Laboratory study on soil behavior in loess slope subjected to infiltration. Eng Geol 183:31–38